Conversion of Whispering Gallery Mode to Dipole Mode

Iftikhar Ahmed[1], Eng Huat Khoo[2] and Ching Eng Png [2]
[1]Department of Electrical Engineering,
University of Tabuk, Kingdom of Saudi Arabia
[1]iftikhar.halifax@gmail.com
[2]Department of Electronics and Photonics,
Institute of High Performance Computing, Singapore
[2] (khooeh, pngce)@ihpc.a-star.edu.sg

***Abstract*—Au metallic nanorods are embedded in semiconductor microdisk in such a way that the whispering gallery mode of microdisk converts to dipole mode. For the simulation of Au nanorods, Lorentz-Drude (LD) model and for semiconductor microdisk, a solid state model is incorporated into Maxwell's equations. The solid state model consists of Pauli Exclusion Principle, state filling and dynamical Fermi-Dirac thermalization effects. We study this dipole phenomenon for different materials, pumping current densities and field orientations.**

***Index Terms*—Finite Difference Time Domain (FDTD), Mode, Lorentz-Drude (LD) model, Solid State Model, Dipole, Microdisk.**

I. INTRODUCTION

Before the World War II, most of the antennas were wire type. Later on, with the development of microwave technology, new types and smaller size antennas such as microstrip, phased array radars etc. were introduced. Antennas made it possible to manipulate the electromagnetic field at the interface of radiation waves and devices. For example, an antenna on a mobile phone localizes or converts propagating electromagnetic energy of many fold larger wavelength to a small chip and vice versa. A lot of work has been done and is ongoing in the field of RF/microwave antennas; however, the concept of optical antennas is relatively emerging in physical optics [1-3]. An optical antenna can be defined as a device that converts optical radiations into localized energy and vice versa [2]. The interest in the area is arising because of the increasing demand of high speed data, high field enhancement, strong field localization and large absorption cross-sections. The fabrication of antennas at optical frequencies was a challenge couple of years ago. The reason was requirement of very small dimensions at these frequencies. Recently, innovative developments in fabrications technologies and emerging areas of nanophotonics and plasmonics have made it possible to fabricate antennas in the optical domain. How to transform well established antenna technology in microwave domain to optical domain is under study field worldwide [2-3]. At radio frequencies (RF), metals have very large conductivities and act as almost perfect reflectors, and perturbation at these frequencies is known as skin depth and is negligible as compared to the antenna dimensions. On the other hand, at optical frequencies, field perturbation or skin depth is up to few tens of nanometer due to plasmonic phenomena, and is comparable to antenna dimensions. This discrepancy results in different design rules for each domain. The diffraction limit in optical domain was another impediment in the miniaturization of devices; it has been eradicated by using the plasmonics effects. Plasmonics deals with electromagnetic wave propagation at the interface of a metal and dielectric. It has made possible nowadays to observe new phenomena at nanoscale and to study the optical fields with nano-antennas. Although study in the areas of optical antennas is still in its infancy, some interesting applications have been and may be developed to enhance the efficiency of existing devices, e.g., efficiency enhancement of LEDs, photovolatics, biosensors and spectroscopy etc. [2-3]. Optical antenna effects in semiconducting GaP nanowires have been studied in [4], where discrete-dipole approximation approach has been used for the simulation of nanowires. Optical dipole nanoantennas can be used to couple radiation to or from optical waveguide (optical fiber), just like radio wave systems [5]. Geometry of antenna structure plays an important role to generate different modes, e.g., non-local effects and shape of metallic nanoparticles can generate, not only the transverse but also longitudinal plasmonics modes [6]. Due to higher momentum of photons, the enhancement in near field also enhances the field absorption in particles [7]. By embedding such metallic nanoparticles or nanorods into semiconductor materials, different phenomena can be observed. As an example, in this paper, plasmonic effect generated by gold nanorods is used to convert whispering gallery mode of a microdisk into dipole mode, and as a result microdisk behaves like a dipole antenna.

For modeling and simulation of optical antennas and devices, different frequency and time domain numerical methods can be used. The frequency domain methods such as method of moments (MoM) [8], finite element method (FEM) [9]; and time domain methods such as FDTD [10], transmission line matrix (TLM) [11], alternating direction implicit (ADI)-FDTD [12] and locally one dimensional

(LOD)-FDTD [13] methods are of interest for such problems. In this paper, the FDTD method is adopted due to its simplicity and generality to simulate the mode conversion phenomenon at optical frequencies. The effect of field absorption into metals cannot be ignored at optical frequencies and many metals show the dispersive nature. The free electrons at the metal surface oscillate collectively at these frequencies and as a result can affect the surrounding media. Here, we consider a microdisk with embedded gold nanorods (GNRs), and to simulate dispersive nature of GNRs LD model is incorporated into Maxwell's equations.

For the simulation of semiconductor microdisk, a solid state model that includes Pauli Exclusion Principle, state filling and dynamical Fermi-Dirac thermalization effects [14-15] is incorporated into Maxwell equations. These both approaches are hybridized to observe the mode conversion phenomenon. The methodology and numerical results are discussed in the subsequent sections.

II. METHODOLOGY

Many materials at optical frequencies show interesting properties and can be simulated by using different models and principles. In this paper, gold and GaAs materials are considered to observe different phenomena. For the modeling of gold, LD dispersive model and for the modeling of GaAs, solid state model is adopted, and both are incorporated into Maxwell's equations. At optical frequencies gold permittivity is frequency dependent, and therefore, Maxwell's equations with frequency dependent permittivity are written as

$$\nabla \times H = \varepsilon_0 \varepsilon(\omega) \frac{\partial E}{\partial t} \tag{1}$$

$$\nabla \times E = -\mu_\circ \mu_r \frac{\partial H}{\partial t} \tag{2}$$

As mentioned earlier, the frequency dependent permittivity is treated by using the Lorentz-Drude model, and to make it consistent with time domain Maxwell's equations, auxiliary differential equation (ADE) approach [14] is used. The LD model consists of two sections, Lorentz and Drude, to capture the dispersive nature of metals [14] [16]. The Drude section is used to deal with free electrons, while the Lorentz section is used to deal with bounded electrons, of gold. After incorporating the LD model in equation (1), and then by applying the ADE approach, following equations are obtained:

$$\frac{\partial E}{\partial t} = \frac{1}{\varepsilon_0 \varepsilon_\infty} \nabla \times H - \frac{1}{\varepsilon_0 \varepsilon_\infty} J_d - \frac{1}{\varepsilon_\infty} \frac{\partial Q_L}{\partial t} \tag{3}$$

$$\frac{\partial J_d}{\partial t} = \omega_{pd}^2 \varepsilon_0 E - Jd\Gamma_d \tag{4}$$

$$\frac{\partial^2 Q_L}{\partial t^2} = \Delta\varepsilon_L \omega_{pL}^2 E - \Gamma_L \frac{\partial Q_L}{\partial t} - \omega_L^2 Q_L \tag{5}$$

where the terms with subscript d represent Drude model while the terms with subscript L represent Lorentz model.

For the simulation of semiconductor material e.g., GaAs, a solid state model that consists of different principles and effects of physics is incorporated into equation (1) and it is modified as

$$\nabla \times H = \varepsilon_0 n^2 \frac{\partial E}{\partial t} - \frac{\partial P}{\partial t} \tag{6}$$

where n represents the refractive index and the term P represents polarizations of the material. The polarization term is calculated by using the expression

$$P = U_m \sum_h N_{dip\_h} \tag{7}$$

where, U_m represents atomic dipole moment, h represents number of levels and N_{dip_h} (number of dipoles divided by unit volume) represents dipole volume density for level h. In other words, the macroscopic polarization is obtained by multiplying the atomic dipole moment and dipole volume density. The atomic dipole moment can be obtained by using the following relation $|U_m|^2 = 3\pi h \varepsilon_o c^3 / \omega_{am}^3 \tau_m$, where h is Planck's constant, c is speed of light, ω_{am} is inter-band transition frequency, τ_m is inter-band transition time.

In the solid state model, the conduction and valence bands are discretized into different and equal numbers of energy levels. The higher the number of discretized energy levels, the higher will be the accuracy [15]. To cover the substantial physics, different principles and effects such as electrical pumping, Pauli Exclusion Principle, Fermi-Dirac thermalization, and electrons dynamics in conduction and valance band, rate equations are included in the solid state model. By hybridizing the both metallic (LD model) and semiconductor (solid state model) approaches active devices can be simulated and interesting phenomena can be discovered [14]. In next section, the hybrid approach is applied to microdisk and gold nanorods to study the mode conversion phenomenon.

III. NUMERICAL RESULTS

For numerical results different numerical experiments are conducted on a GaAs microdisk of radius R = 700 nm, and thickness H = 196 nm. Four gold nanorods (GNRs), each having a radius r and height h are embedded in the microdisk. Different values of r and h are considered for analysis. The gold nanorods are selected because they have less oxidation tendency as compared to the silver nanorods. The 3D, side and top views of the disk with GNRs are shown in Fig. 1. Parameters for gold rods are $\omega_{pD} = 2\pi \times 1903.41 \times 10^{12}$ rad/sec, $\Gamma_D = 2\pi \times 12.81 \times 10^{12}$ rad/sec, $\Gamma_L = 2\pi \times 58.27 \times 10^{12}$ rad/sec, $\varepsilon_\infty = 1$.

For GaAs microdisk, the effective mass of electrons for conduction band is $.046\, m_e$, whereas the effective mass of hole for the valance band is $.36\, m_e$, m_e is mass of electron in free space. The numbers of energy levels h taken for conduction and valance bands are 10, and the carrier density is 8 x 10^{22} m^{-3}.The refractive index is 3.54, whereas the

transition parameters are adopted from [17]. The pumping rate is $3x10^9$/s.

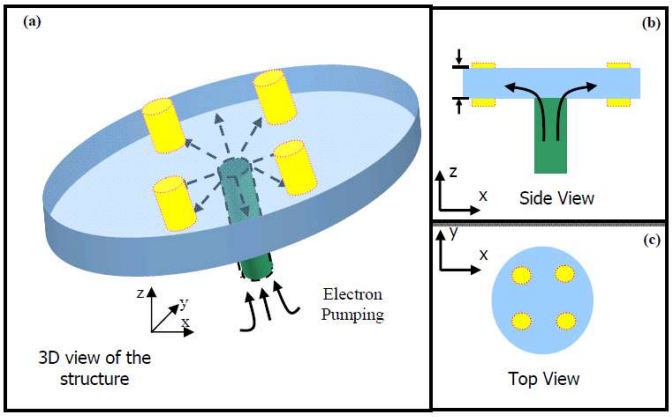

Fig. 1. Schematic of GaAs microdisk with four embedded gold nanorods.

These parameters are taken at room temperature and a Gaussian pulse is used as a source. Fig.2 (a)-(f) show the field patterns of conventional microdisk, and with four GNRs of different radii *r* and heights *h* embedded in microdisk. Fig. 2 (a) indicates the electric field pattern of the conventional microdisk, and is in the form of whispering gallery mode. For the observation of different phenomena GNRs are used inside the microdisk as shown in Fig.1. Fig.2 (b) demonstrates the field pattern with four embedded gold nanorods. The radius and height of each nanorod is 112 nm and 252 nm respectively. It indicates that the microdisk is behaving like a dipole antenna. It radiates at angles 135° and -45°. It is conspicuous that the whispering gallery mode exploits the unique properties of the gold nanorods (plasmonics effect) at optical frequencies. Each nanorod starts behaving like a source due to highly localized field around them, and as a result stimulates light matter interaction. In addition, at near field, photon momentum is comparable to electron momentum owing to strong spatial confinement of field around gold nanorods. These factors affect charge carriers in the semiconductor microdisk and as a result to dipole volume density N_{dip_h}. Consequently, at optimized dimensions of nanorods, whispering gallery mode transform to dipole mode. Field along nanorods propagates in both longitudinal and transverse directions, while the transverse direction field oscillates in the radial direction and affects the electron movement more strongly as compared to longitudinal direction. These factors influence the dipole moments and as a result to polarization, and there by lead to the dipole phenomenon.

The Hamiltonians (*H*) of the system (sum of all the possible energies of particles in a system) that play an important role in the mode conversion are

$$H = H_p + H_f + H_b + H_{WGM} \quad (8)$$

where H_p is a Hamiltonian related to pumping electrons; H_f is linked to free electron along the surface of GNRs; H_b represents bounded electrons; and H_{WGM} is Hamiltonian due to boundaries or whispering gallery mode. Under the dipole condition, the H_{WGM} is negligibly small, while the others Hamiltonians play a dominant role. H_f is negligible for the case of the conventional microdisk and the rest generate whispering galley mode. Drude model capture the free electrons effect at the surface of nanorods, Lorentz model accommodate the bounded electrons or dipole moments inside the GNRs. The Hamiltonian H_f is linked to Drude model and free pumping electrons, whereas H_b is linked with oscillation of bounded electrons in microdisk and Lorentz model. In the active model the effect of electron pumping and dipole moments of the semiconductor cavity are considered through the polarization term for the analysis of structure.

At the resonance wavelength, at which the disk behaves like a dipole antenna, the field is aligned in dipole fashion as depicted in Fig. 2 (b) and (f). It is noticed that in the case of Fig. 2 (b), the field is negligibly small along the 45° and 225°, and similarly along 135° and -45°, if the direction of source excitation is reversed as shown in Fig. 2 (f). For further numerical experiments, we have varied the *r* and *h* of the nanorods and have observed different field patterns, as compared to that shown in Fig. 2 (b).

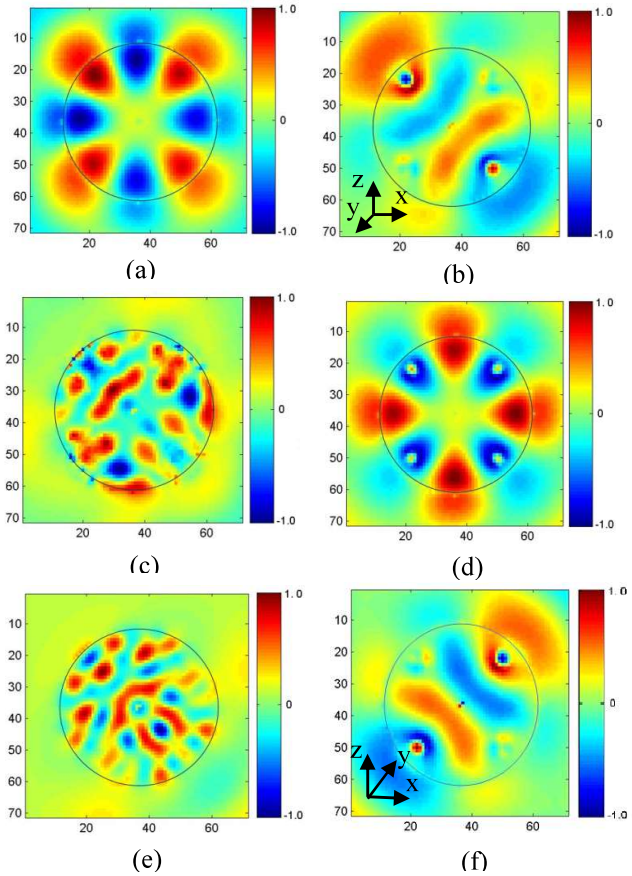

Fig. 2. Electric field pattern for different height and width of nanorods at steady state; (a) conventional microdisk; (b-f) with four nanorods of different radii and heights embedded in the microdisk.

Fig. 2 (c) depicts the field pattern when the radius of nanorods is 224 nm and the height is 252 nm. It doesn't

show either whispering gallery modes or dipole pattern instead a random pattern or noise. The reason of this is *r* and plasmonics effects of gold nanorods. The area of field oscillation around the nanorods increases due to larger *r* as compared to the dipole pattern case and it disturb the movement of electrons as compared to the regular pattern inside the disk. In this case, some other modes are also observed in addition to the dominant mode, and these additional modes appear because of field scattered from the nanorods for certain given dimensions, and because of roughness of cavity surface, etc. Fig. 2 (d) shows the field pattern when the radius and height of the nanorods are 84 nm and 252 nm, respectively. This case does not exhibit the dipole nature, instead shows a quadpole nature and a suppression of the field around the GNRs. It is because of the smaller *r* and, as a result, smaller resonance region around the rods. This does not affect the field radiation along vertical and horizontal axis of the microdisk.

Fig. 2 (e) depicts the pattern when the r = 84nm and h = 280 nm. We do not observe any whispering gallery mode, or dipole mode, and the reason is the scattering and oscillation of the free electrons around the nanorods, both inside and just above the micordisk. The effect of the field in radial direction is smaller, similar to Fig. 2 (d), owing to the fact that the radius is the same. However, the height of the rods is higher in the air and, as a result, the radial field oscillation range is also larger. This acts like an external source on the surface of disk and suppresses the WGM and dipole modes. Fig. 2 (f) shows the dipole nature of the disk but in the opposite direction to that of the Fig. 2 (b). In this case, fields radiates along 45^o and 225^o , because of the direction of excitation source as indicated in subplot, which is opposite to that of Fig. 2 (b). The coupling of plasmonic and whispering gallery modes in microdisk leads to antenna operating in the dipole mode under the condition that dimensions of GNRs are optimized.

Fig. 3 illustrates the normalized electric field intensity with respect to wavelength for different heights and radii of the nanorods inside the microdisk. It is conspicuous to see from Fig. 3, how the different dimensions of the nanorods affect the resonance wavelength. The resonance wavelength of the conventional disk is 634.4 nm and the corresponding field pattern is shown in Fig. 2 (a). The resonance at which the disk shows dipole antenna behavior is 670.1 nm. It explains why the wavelength shift during the conversion of the whispering gallery mode to the dipole mode is 35.7 nm. However, when the radius or heights of the nanorods are changed, we observed some noise that affects the field and dipole nature of the disk. When the h of nanorods is 280 nm, and the radius is 84 nm, the height affects the resonance wavelength and causes more noise, although in this case the effect of radius is less. The different resonance peaks in Fig. 3 show that there exist numbers of modes inside the disk. This noise is present because of electrons oscillation around nanorods in free space just above the microdisk and that affect the resonance wavelength. Similarly, when r = 224 nm, the effect of the noise is less severe as compared to the case of larger heights of the rods. This observation is clear from Fig. 3, which shows less resonance peaks as compared to the previous case, although there is no clear separation between the WGM and dipole modes. Numerical experiments show that the dipole phenomena can be observed in a microdisk only for the optimized radii and heights of the nanorods.

For the case of dipole pattern, the height and width of the nanorods is optimized and the plasmonic effect due to gold rods guides the field in dipole fashion. The field pattern in Fig. 2 and the plot in Fig. 3 also show that only the main mode is dominant and the others are suppressed due to electron oscillation around the gold nanorods. The distance between the GNRs also plays an important role, which changes with the changes in the diameters of the GNRs. The area of the field resonance around them also changes, which affects the interferences of the fields with neighboring GNRs. This interference distorts the WGM and vice versa, as appears from Figs. 2 (c) and 2 (e). There is less interaction between the localized fields between the GNRs if the distance between them is larger and the result is shown in Fig. 2 (d), at optimized distances the field pattern changes to the dipole modes.

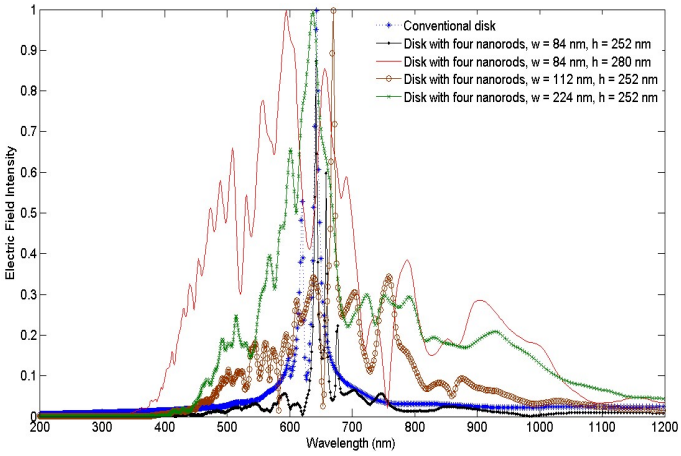

Fig. 3. Normalized electric field intensity with respect to wavelength for different radii and heights of nanorods.

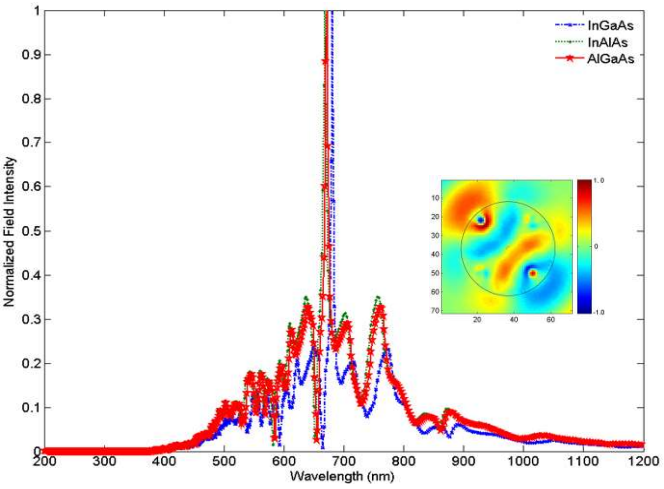

Fig. 4. Electric field intensity with respect to wavelength for different materials.

Different materials such as InGaAs, InAlAs and AlGaAs have been used for microdisk to observe the dipole

phenomena with the same set up as in Fig.1. The reason for using different materials is their usability in different environments. The *r* and *h* of the nanorods, and the thickness and radius of the disk are same as used for Figs. 2 (b) and (f). All of them show the dipole nature, though at different wavelengths, as expected due to different refractive index, effective mass for holes and electrons. The results are shown in Fig. 4. Fig. 5 indicates the normalized field intensity with respect to pumping current density for the structure under study. With the increase in current density, field intensity also increases but it saturates after certain amount of current values as shown in Fig. 5.

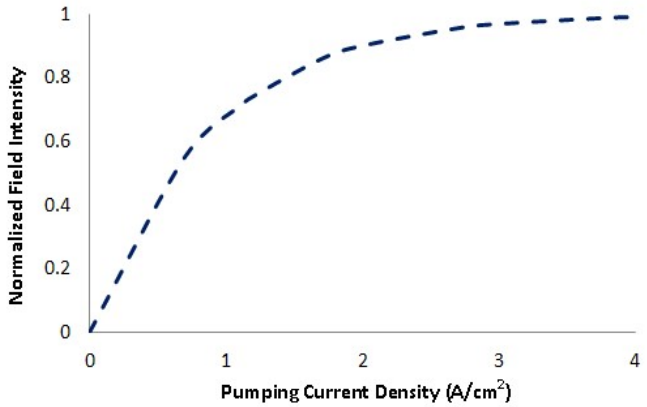

Fig. 5. Field intensity with respect to pumping current density

IV. CONCLUSIONS

It is found that by using the optimized dimensions of the gold nanorods, the whispering gallery mode in a microdisk can be converted to a dipole mode, by changing the field excitation direction, light are radiated in the opposite direction. The interaction of the enhanced electromagnetic field with pumping electrons in the microcavity enhances the potential energy of the systems. This change in the potential affects the dipole moment, intraband and interband transition of the electrons, and leads different pattern and wavelength of the resonance mode. Different materials for microdisk have been considered to study the phenomenon and the results are found to be very promising, because this development may have applications in the field of sensing, e.g., biosensing and in optical near-field applications.

REFERENCES

[1] D. K. Cheng, "*Field and wave electromagnetics*", Second Edition, Addison-Wesley Publishing Company, Inc. 1992

[2] P. Bharadwaj, B. Deutsch and L. Novotny, " Optical antennas", *Advances in Optics and Photonics,* vol. 1, pp. 438-483

[3] Q. H. Park, " Optical antennas and plasmonics", arXiv:0901.2162v1 *physics.optics*, 2009

[4] G. Chen, Jian Wu, Qiujie Lu, H. R. Gutierrez, Qihua Xiong, M. E. Pellen, J. S. Petko, D. H. Werner, and P. C. Eklund , "Optical Antenna Effect in Semiconducting Nanowires" *Nano Letters*, 2008, Vol. 8, No. 5 1341-1346

[5] A. Andryieuski, R. Malureanu, G. Biagi, T. Holmgaard and A. Lavrinenk, "Compact dipole nanoantenna coupler to plasmonic slot waveguide", *Optics Letters* Vol. 37, No. 6 , 1124-1126, 2012

[6] H-Y. Xie, M-Y. Ng, and Y-C. Chang, "Analytical solutions to light scattering by plasmonic nanoparticles with nearly spherical shape and nonlocal effect, *J. Opt. Soc. Am. A* , Vol. 27, No. 11, 2411- 2422, 2010

[7] V. M. Shalaev, "Electromagnetic properties of small-particle composites," Phys. Rep. 272, 61–137 (1996).

[8] R. F. Harrington, *Field Computation by Moment Methods,* Wiley-IEEE Press, 1993.

[9] J. Jin, *The Finite Element Method in Electromagnetics*, 2nd. ed.. Wiley-IEEE Press, 2002.

[10] A. Taflove and S. C. Hagness. *Computational Electrodynamics: The Finite-Difference Time-Domain Method*, 3rd ed.. Artech House Publishers, 2005.

[11] W. J. R. Hoefer, "The transmission-line matrix method theory and applications", *IEEE Trans. Micro. Theory Tech,* Vol. 33, No. 10, pp. 882-892, 1985

[12] F. Zheng, Z. Chen, and J. Zhang, "A finite-difference time-domain method without the Courant stability conditions," *IEEE Microw. Guided Wave Lett.*, vol. 9, no. 11, pp. 441–443, 1999.

[13] I. Ahmed, E. K. Chua, E. P. Li, and Z. Chen, "Development of the three dimensional unconditionally stable LOD-FDTD method," *IEEE Trans. Antenna Propag.,* vol. 56, no. 11, pp. 3596–3600, 2008.

[14] I. Ahmed, E. H. Khoo, O. Kurniawan and E. P. Li "Modeling and simulation of active plasmonics with the FDTD method by using solid state and Lorentz-Drude dispersive model", *Journal of Optical Society America B*, Vol. 28, pp..352-359, 2011.

[15] Y. Huang , and S. T. Ho, "Computational model of solid state, molecular, or atomic media for FDTD simulation-based on a multi-level multi-electron system governed by Pauli exclusion and Fermi–Dirac thermalization with application to semiconductor photonics*," Opt. Exp*., vol. 14, pp. 3569–3587, 2006.

[16] D. Rakic, A. B. Djurisic, J. M. Elazar and M. L. Majewski "Optical properties of Metallic films for vertical-cavity optoelectronic devices" *Apl. Optics.* 37, 5271-5283, (1998).

[17] S. Marrin, B. Deveaud, F. Clerot, K. Fuliwara, and K. Mitsunaga, "Capture of photoexcited carriers in a single quantum well with different confinement structures," *IEEE J. Quantum Electron*. 27, 1669-1675, (1991).

AUTORS BIOS

IFTIKHAR AHMED received PhD degree in Electrical Engineering from Dalhousie University, Canada. Currently, he is an associate professor in the Department of Electrical Engineering at University of Tabuk, Kingdom of Saudi Arabia.

Previously, he was a scientist and capability group manager in the Department Electronics and Photonics at A*STAR Institute of High Performance Computing, Singapore. He is a senior member of IEEE and member of different societies. He has won numerous awards, authored and coauthored over 75 journal and conference papers, and three book chapters. His research interest includes computational electromagnetics from RF/microwave to optical frequencies and from macro to nanometer size applications.

E. H. Khoo received the B.Eng degree (with honours) and Ph.D degree in electrical and electronics engineering from the Nanyang Technological University, Singapore in 2003 and 2008, respectively. He is currently in Institute of High Performance Computing as a research scientist. His current research interests include plasmonics, passive and active photonic, computational algorithm and solid state physics. He has author over 30 journal papers and more than 50 conference papers.

Ching Eng (Jason) Png received his Ph.D and executive MBA degree from Surrey University, INSEAD and Tsinghua University respectively. Dr. Jason Png is currently Director of Electronics & Photonics at IHPC, A*STAR where he leads a number of exciting projects as principal investigator. He won a number of awards for his research in photonics, including the prestigious Royal Academy of Engineering Prize in London, UK, and has delivered invited talks including at IBM's Research Division in the USA. Additionally, he is a member of the A*STAR Early Career Advisory Committee. He actively volunteers in national scientific competitions. Dr. Png was an Adjunct Assistant Professor at NUS.